Environmental Pollution 334 (2023) 122033

Contents lists available at ScienceDirect

Environmental Pollution

journal homepage: www.elsevier.com/locate/envpol

How efficiently does a metabolically enhanced system with denitrifying anaerobic methane oxidizing microorganisms remove antibiotics?☆

Silvana Quiton-Tapia *, Sabela Balboa, Francisco Omil, Juan Manuel Garrido, Sonia Suarez

CRETUS Institute. Department of Chemical Engineering, School of Engineering, Universidade de Santiago de Compostela, Rúa Lope Gómez de Marzoa, E-15782, Santiago de Compostela, Spain

ARTICLE INFO

Keywords:
Organic micropollutants
N-Damo bacteria
Specific biomass activity
Anoxic conditions
Removal of antibiotics

ABSTRACT

In this work, the novel N-damo (Nitrite dependent anaerobic methane oxidation) process was investigated at high biomass activities for its potential to remove simultaneously nitrite and methane, as well as selected antibiotics commonly found in sewage in trace amounts. For this purpose, two MBRs were operated at three high nitrite loading rates (NLRs), namely 76 ± 9.9, 161.5 ± 11.4 and 215.2 ± 24.2 mg $N–NO^-_2$ L^{-1} d^{-1}, at long-term operation. The MBRs performance achieved a significantly high nitrite removal activity for an N-damo process (specific denitrifying activity of up to 540 mg $N–NO^-_2$ g^{-1} VSS d^{-1}), even comparable to heterotrophic denitrification values. In this study, we have implemented a novel operational strategy that sets our work apart from previous studies with similar bioreactors. Specifically, we have introduced Cerium as a trace element in the feeding medium, which serves as a key differentiating factor. It allowed maintaining a stable reactor operation at high NLRs. Microbial community composition evidenced that both MBRs were dominated with N-damo bacteria (67–87% relative abundance in period III and I, respectively). However, a decrease in functional N-damo bacteria (*Candidatus Methylomirabilis*) abundance was observed during the increase in biomass activity and concentration, concomitantly with an increase of the other minor families (*Hypomicrobiaceae* and *Xanthobacteraceae)*. Most of the selected antibiotics showed high biotransformation such as sulfamethoxazole, trimethoprim, cefalexin and azithromycin, whereas others such as roxithromycin and clarithromycin were only partially degraded (20–35%). On the contrary, ciprofloxacin showed almost no removal. Despite the metabolic enhancement, no apparent increase on the antibiotic removal was observed throughout the operation, suggesting that microbiological composition was of greater influence than its primary metabolic activity on the removal of antibiotics.

1. Introduction

Nitrite dependent anaerobic methane oxidation (N-damo) is a microbial process with promising technological features for sustainable nitrogen removal in wastewater treatment (van Kessel et al., 2018). The particularity of the N-damo process is the capability to remove methane and nitrogen simultaneously without the emission of nitrous oxide as an intermediate (Equation (1)). As a result, two important Greenhouse Gases (GHGs) (i.e. methane and nitrous oxide), are mitigated during this process (Stein, 2020). The nitrite removal is catalyzed by bacteria associated to the NC10 phylum, identified with the genus *Candidatus* Methylomirabilis (Ettwig et al., 2010). This technology is particularly relevant for wastewater treatment plants (WWTPs) based on anaerobic processes, because they produce effluents with high dissolved methane concentrations, specially at low to moderate temperatures (Sánchez et al., 2016).

$$3CH_4 + 8NO^-_2 + 8H^+ \rightarrow 3CO_2 + 4N_2 + 10H_2O \quad \left(\Delta G^\circ = -928 \text{ kJ mol}^{-1}\ CH_4\right) \tag{1}$$

The challenge is achieving stable application of N-damo processes at relevant activities. Previous studies reported low (Chang et al., 2021) and even decreasing values in long-term reactor operation with no proven reason (Kampman et al., 2012), mainly explained by the low doubling times of N-damo microorganisms (up to 2 weeks) (Ettwig et al., 2010), as well as oxygen and nitrite inhibition (Arias et al., 2022;

☆ This paper has been recommended for acceptance by Meththika Vithanage.

* Corresponding author.
E-mail addresses: silvanaines.quiton@usc.es (S. Quiton-Tapia), sabela.balboa@usc.es (S. Balboa), francisco.omil@usc.es (F. Omil), juanmanuel.garrido@usc.es (J.M. Garrido), sonia.suarez@usc.es (S. Suarez).

https://doi.org/10.1016/j.envpol.2023.122033
Received 12 April 2023; Received in revised form 26 May 2023; Accepted 10 June 2023
Available online 21 June 2023

Luesken et al., 2011). Previous enrichment experiments showed specific nitrite activity as low as 2 mg N g^{-1} VSS d^{-1} (He et al., 2015b). Recent N-damo works using MBRs showed a significative increase in activities with values between 64 (Arias et al., 2022) and 95 mg N g^{-1} VSS d^{-1} (Allegue et al., 2018).

Despite the technological advancements on the N-damo process, the reported specific activities are far below those corresponding to heterotrophic denitrification and anammox biomass (Lotti et al., 2015; Metcalf & Eddy et al., 2014). This fact might limit, among others, the practical development of N-damo bioreactors to treat wastewater One strategy for increasing the capacity of N-damo bioreactors, could be the modification of the feed medium by adding trace amounts of lanthanides such as Cerium (Ce), as suggested by some authors (Guerrero-Cruz et al., 2019; Versantvoort et al., 2018).

In addition to the removal capacity of nitrogen and methane, new WWTPs also need to consider the removal efficiency of Organic Micropollutants (OMPs). The OMP biotransformation potential is determined by the specialized microbial community present in biological systems (Wolff et al., 2018). This biotransformation mechanism can be performed by a metabolic or cometabolic process, although the latter was more often reported due to the relatively low OMP concentrations in the environment (Tran et al., 2013).

Previous research has shown that the increase in primary substrate is an effective operational strategy to enhance OMP removal, as higher biomass activities correlate with OMP biotransformation (Alvarino et al., 2014; Kennes-Veiga et al., 2021; Martínez-Quintela et al., 2021). Accordingly, the N-damo process has shown evidence of cometabolic biotransformation of several OMPs, including antibiotics (Martínez-Quintela et al., 2021). In the latter research, a cometabolic removal was suggested by the correlation between increasing specific nitrite removal rates and OMP removal, with a maximum nitrite removal rate of 59 mg $N.L^{-1}d^{-1}$. However, the relationship between primary metabolism and cometabolic OMP removal is complex and not always follows a positive correlation, as it is suggested that cometabolism has a lower (activation) and upper limit (saturation) (Sheng et al., 2021). In this sense, it is still unclear if a cometabolic tendency is still observed during high N-damo activities.

The aim of this work was to metabolically enhance the N-damo process to reveal if high and steady N-damo activities can promote the biotransformation of a selected group of antibiotics during long-term operation. To this end, we progressively increased the Nitrogen Loading Rate (NLR) and adapted the micronutrients content by the addition of Cerium. Our results provide insights on the influence of primary substrate on the potential biotransformation capacity of N-damo microorganisms, as well as understanding the microbiological implications of the effect of NLRs and antibiotic presence by evaluating shifts on the microbial community composition.

2. Materials and methods

2.1. Reactor configuration and continuous-flow operation

Two analogous MBRs, MBR1 and MBR2, each with 10 L capacity and a working volume 6.65 L, were operated in parallel at stable conditions in a similar configuration as described in Allegue et al. (2018). Both MBRs had a submerged hollow-fiber ultrafiltration membrane module (Puron) with a 0.5 m^2 surface and a pore size of 0.03 μm. The membrane cycle operation consisted of 7 min of permeation and 30s of relaxation. The system continuously measured transmembrane pressures using a pressure sensor PN 2069. No back flushing was performed during the reactor operation, but frequent biomass resuspension with nitrogen gas was performed to avoid biomass accumulation in the membrane. Additionally, the Oxidation-Reduction Potential (ORP) inside each MBR were measured in real-time by using a redox probe Hamilton Polyplast ORP BCN. All sensors were connected to a programable PLC Micro 820 (Allen-Bradley) for real-time control. The HRT was maintained at ~1 day and the temperature was fixed at 28 °C using a thermostatic water bath.

The inoculum used had been subject to previous N-damo enrichment strategies for more than 3 years (Allegue et al., 2018; Arias et al., 2022; Martínez-Quintela et al., 2021). It was analyzed through 16 S rRNA metabarcoding sequencing that evidenced a maximum abundance of N-damo phylum of around 30–50%, mainly represented by the *Methylomirabilaceae* family.

The system was fed with synthetic wastewater containing sodium nitrite as nitrogen source and a mixture of macronutrients and trace compounds according to Arias et al. (2022) (Table A1). Cerium (Ce) was included as trace element to promote the growth of N-damo bacteria (Versantvoort et al., 2018) and other methanotrophic microorganisms associated to N-damo cultures (Pol et al., 2014). Methane was fed continuously in saturation as a gas mixture CH_4 and CO_2 90:10%. The gas volume was adjusted in function of the biomass activity and NLR as the CO_2 was used for pH control. The pH was measured in the feed and permeate daily using a Hach pH probe. The gas was recirculated from bottom to the top using a mini laboratory blower N86 KT 18 (Laboport) for mixing purposes and prevention of membrane fouling. The gas volume was quantified by using a Mili GasCounter MGC-1V3.3 PMMA (Ritter).

2.2. Operational strategy

The two MBRs were operated in parallel during three experimental periods defined by the applied NLRs: 70 (PI), 140 (PII) and 220 (PIII) mg $N–NO^-_2L^{-1}$. The only difference was that a continuous mix of antibiotics was fed only to MBR2. Thus, MBR1 was used as a microbial control to evaluate separately the influence of increasing the NLR in the microbial composition. Once the system reached a steady state, samples were taken to evaluate the antibiotic removal in MBR2 as well as the microbial composition in MBR1 and MBR2.

2.3. Selected OMPs

A mixture of seven OMP at a final concentration of 5 μg L^{-1} was fed to MBR2. Compounds were selected based on their occurrence in sewage, persistence in the environment and their high priority to monitor by the European legislation (Watch List, WFD, 2000/60/EC). The selected substances correspond to four classes of antibiotics: cephalexin (CFX) as a representative of the group of cephalosporins; sulfamethoxazole (SMX) a widely used sulfonamide, usually combined with trimethoprim (TMP); ciprofloxacin (CIP) as a member of fluoroquinolones and the macrolides roxithromycin (ROX), azithromycin (AZY) and clarithromycin (CLA).

2.4. Analytical methods

Nitrogen species were determined by spectrophotometric measurements. Solids were only measured extracting mixed liquor biomass directly from the MBRs as no solids were found in the permeate due to the membrane retention Biomass concentration was measured by extracting 10 mL of mixed liquor from the MBRs. Total suspended solids (TSS) were quantified by weighting the solid fraction after 0.45 μm filtration using a glass fiber filter. Consequently, volatile suspended solids (VSS) accounted for the remaining solids after the muffle oven at 550 °C for 30 min as indicated in the standard methods (APHA, 2000).

Total organic carbon (TOC) was measured following the method 5310 from the Standard Methods (APHA, 2000), using a Shimadzu TOC-L CSN. The method measures TOC in an indirect way by determining the difference between Total Carbon (CT) and Inorganic Carbon (CI). The trace element composition was measured in each experimental period in the liquid feed and permeate using inductively coupled plasma mass spectrometry (ICP-MS).

The gas volume fed to each reactor was quantified using a Mili

GasCounter MGC-1V3.3 PMMA (Ritter). The system also had an online Ultramat 23 gas analyzer (Siemens) to detect the presence of nitrous oxide. Additionally, the gas composition (nitrogen gas, carbon dioxide and nitrous oxide) was determined periodically by using a gas chromatograph (HP 5890 Series II).

Antibiotic removal efficiencies were determined by analyzing their concentrations in the aqueous phase of the influent and permeate from MBR2. Sorption was not considered as a relevant removal mechanism due to the low lipophilicity of the compounds selected. Three antibiotic sampling campaigns were performed for each experimental period (n = 9). All replicates were analyzed for data quality control according to average values and standard deviation, outliers were excluded from further analysis.

All samples were collected in amber glass bottles and immediately filtered at 0.45 μm with an initial volume of 200 mL. Afterwards, samples were preconcentrated using Solid Phase Extraction (SPE) as indicated in Gros et al. (2013) and later quantified by using a liquid chromatograph Agilent 6410 B-QQQ LC/MS. The column used was C18 Zorbax eclipse XDB 2,1 × 150mmx5μm. The solvents for Phase A were 10 mM of formic acid/ammonium formate and for Phase B: Methanol. Each injection used 20 μl of sample.

2.5. Microbiological analysis

Biomass samples were taken from the MBRs during steady operation, after resuspension with nitrogen gas. Subsequently, genomic DNA was extracted by triplicate using the Nucleospin Microbial DNA extraction kit (Machery-Nagel). The replicas from each sample were pooled together after quantification, and quality control using Nanodrop and Qubit fluorometer (Thermo Fisher Scientific Waltham, MA, USA). The V3–V4 hypervariable region for Bacteria was amplified using Bakt_341 F (5′ CCT ACG GGN GGC WGC AG 3′) and Bakt_805 R (5′ GAC TAC HVG GGT ATC TAA TCC 3'). DNA metabarcoding analyses of the region were carried out in an Illumina NovaSeq PE250 platform, generating paired ends reads (2 x 250) by All Genetics & Biology SL (www.allgenetics.eu).

Bioinformatic analyses were performed using the Microbial Genomics module (version 21.1) workflow of the CLC Genomics workbench (version 21.0.3). Raw sequences were filtered and then clustered into Operational Taxonomic Units (OTUs) at 97% cutoff for sequence similarity and classified against the non-redundant version SILVA SSU reference taxonomy (release 132; http://www.arb-silva.de). Only the most abundant bacterial OTUs (above 1% of the total observed OTUs) were considered for further analysis.

2.6. Activity assays

The maximum activity of the biomass was determined by a single "in situ" batch assay once the reactor reached a stable operation in each of the three experimental periods (PI, PII and PIII). The liquid feed was disconnected, and a nitrite pulse was added to the reactors. Degradation kinetics were followed with time until there was no nitrite concentration left.

3. Results and discussion

3.1. MBRs performance

Two anoxic MBR reactors were operated in an analogous way for 234 days divided in three experimental periods defined by different nitrite loading rate (NLR) (Table 1). The operation was characterized by a stable hydraulic performance in both reactors and robustness of the system to reach and maintain the different high NLRs. The HRT for MBR1 was 1.04 ± 0.18 d and for MBR2 was 1.04 ± 0.08 d. Transmembrane pressure was below an average of −39 mbar for both MBRs, but particularly lower for MBR2. The membrane permeability was approximately 35 and 15 L m-2 h-1 bar-1 for MBR1 and MBR2, respectively. Moreover, the system efficiently removed all nitrite fed, reaching NRRs up to 220 mg N– NO_2^- L^{-1} d^{-1} for period III (Table 1). Overall, the average nitrite concentrations in permeates were of 0.9 ± 2.0 and 0.6 ± 1.6 mg N–NO2- L-1 for MBR1 and MBR2, respectively.

Table 1
Different experimental periods and corresponding NLRs for MBRs operation.

Period	Phase	Reactor operation (days)	Nitrite Loading Rate[a] (mg $N–NO_2^-$ L^{-1} d^{-1})	
			MBR1	MBR2
I	Initial load	0–136	68.78 ± 10.24	70.31 ± 10.01
II	Medium load	137–185	162.5 ± 9.6	161.5 ± 11.4
III	High load	186–234	220.1 ± 26.3	215.2 ± 24.2

[a] Average values for the whole period are shown from which standard deviation values were calculated after the reactor reached the desired NLR, excluding the days that the load was progressively being increased (n = 3).

Additionally, nitrate and ammonium concentrations were quantified in both influent and permeate. Ammonium was fed as a macronutrient with average concentrations of 3.27 ± 0.61 and 3.20 ± 0.66 mg N–NH+4 L^{-1} for MBR1 and MBR2 respectively. On the contrary, nitrate was not purposely fed to the system but was found present in concentrations of 3.69 ± 1.71 mg $N–NO_3^-$ L^{-1} for MBR1 and 2.66 ± 1.68 mg $N–NO_3^-$ L^{-1} for MBR2. The presence of nitrate was probably due to the oxidation of nitrite with the remaining oxygen left in the feeding bags after the purging of dissolved oxygen with nitrogen gas. TOC concentrations in the feed had an average value of 3.81 ± 2.42 mg TOC L-1 and 3.73 ± 1.70 mg TOC L-1 for MBR1 and MBR2 respectively, limiting heterotrophic denitrification. As for pH, the system was kept very stable with average values in the permeate of 7.76 ± 0.31 and 7.63 ± 0.35 for MBR1 and MBR2, respectively.

Period I (PI) (days 0–136) included the start-up of the system with a progressive increase of the NLR until a steady operation at 74.7 ± 8.5 and 76.0 ± 9.9 mg NO^-_2-N·L^{-1} for MBR1 and MBR2, respectively (in approximate 20 days). The MBRs steady operation was sustained until day 63, when the antibiotic mixture was added in MBR2 while maintaining analogous operation with MBR1. Then, both MBRs operation was maintained for another 58 days to ensure the biomass acclimation to antibiotics in MBR2 before the first antibiotic campaign (days 122–136). The antibiotic mixture did not show any impact on the reactor performance by means of primary metabolism. During the first days of both MBRs operation, sodium carbonate (in a range of 250–300 mg L^{-1}) was included in the feeding medium to avoid acidification of the bioreactor due to absorption of CO_2 present in the methane-carbon dioxide gas mixture fed to the system. Later, when the denitrifying activity could avoid the acidification of the bioreactor, sodium carbonate addition was discontinued.

Period II (PII) (days 137–185) incorporated the first increase of the nitrite load with a 2.18-fold increase in the NLR within two weeks (going from 79 to 172 mg N–NO-2 L-1 d-1). The maximum biomass concentration in this stage reached 2.98 and 1.49 g VSS L-1 for MBR1 and MBR2, respectively. The increase in biomass concentration accounted for less than 0.12 g VSS for both reactors (Figure A2).

Period III (PIII) (days 186–234) refers to the highest NLR applied. The system swiftly sustained a fast and progressive increase of 60 mg N–NO-2. L-1 d-1 in only 8 days reaching an average NLR of 220.07 ± 26.27 mg N L-1 d-1 for MBR1 and 215.21 ± 24.22 mg N L-1 d-1 for MBR2 (Fig. 1). The steady efficiency of the reactor during the increase in NLR shows the system capacity to adjust to higher nitrite loads. The increase in NLR also had an influence in the biomass concentration. During this period, the biomass in MBR2 doubled, reaching a final concentration of 2.47 g MLVSS from the 1.49 g MLVSS in PII (Figure A2).

The ORP measurements evidenced reducing conditions with average values of - 347.7 ± 135 mV for MBR1 and -197.5 ± 109.5 mV for MBR2.

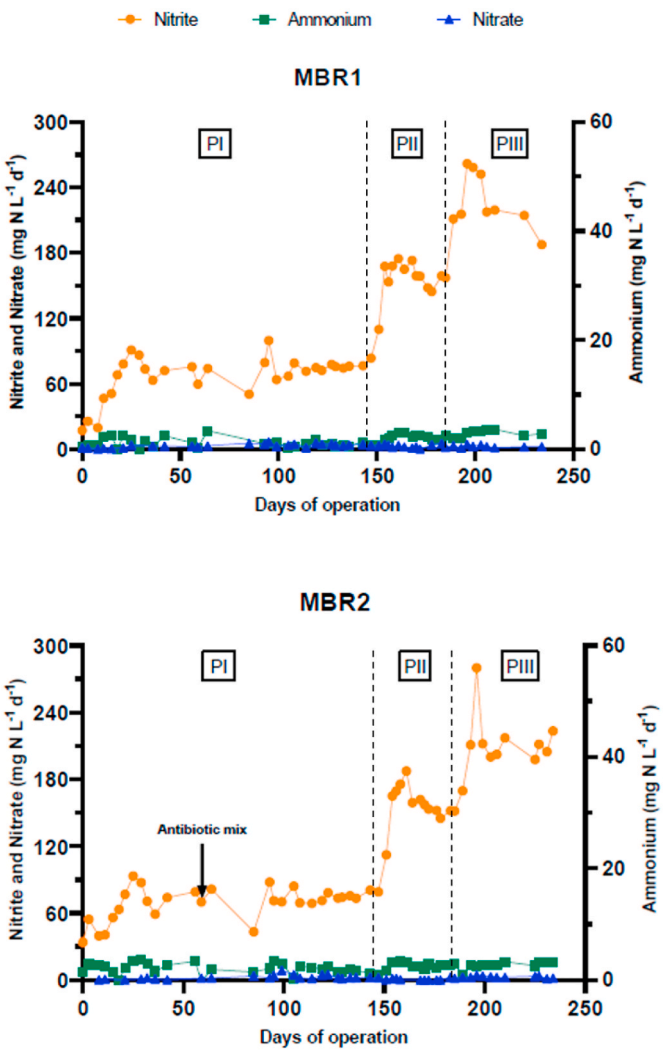

Fig. 1. Volumetric nitrogen rates in MBR1 (above) and MBR2 (below) during the reactor operation. In the left Y axis, nitrite removal as in mg $N–NO^-_2 L^{-1}d^{-1}$ and nitrate removal as in mg $N–NO^-_3$ $L^{-1}d^{-1}$ are shown while ammonium removal is displayed in the right axis as mg $N–NH^+_4$ $L^{-1}d^{-1}$ (n = 3). Experimental periods are separated by dashed vertical lines.

The ORP deviation in both MBRs correlated with abundance and depletion of nitrite and nitrous oxide in the system. The real time values were also dependent on the cycle feed, showing higher values when the reactor was actively receiving the feed. Therefore, redox measurements in real time were used as a nitrite surrogate parameter to quickly identify the system capacity when nitrite was increased.

The removal rates achieved are similar as those evidenced by Arias et al. (2022) and higher than those evidenced in similar MBRs (Allegue et al., 2018; Martínez-Quintela et al., 2021) which supports the assertion of the importance of media composition, in this work by the addition of the lanthanide Cerium, which we link to the observed boosted reactor efficiency. Accordingly, the ICP-MS measurements evidenced that Cerium was completely removed in all experimental periods from the initial concentration fed to the system (Table A1). These results agree with previous research that suggests that methanotrophic and methylotrophic microorganisms, present in N-damo enrich cultures, can employ Ce instead of Calcium as cofactor and ultimately, enhance microbial kinetics (Guerrero-Cruz et al., 2019).

3.1.1. Biomass growth

The apparent doubling time (T_d) and yield (Y) were determined as key physiological properties of the N-damo culture in the highly enriched MBRs. For the T_d quantification, biomass concentration was monitored during the complete operation in both MBRs. In figure A2, the evolution of biomass growth is depicted for MBR2 from an initial concentration of 1.10 g MLVSS. L^{-1} up to a final biomass concentration of 3.08 g MLVSS L^{-1} after an exponential growth in PII and PIII.

The T_d was calculated considering the values for the biomass growth from days 189 till 234 (PII and PIII), which showed the highest biomass increase during the reactor operation (Figure A2). For this purpose, the reaction rate (B) was estimated using a linear equation for an exponential growth model (Equation (2)), from which the intercept (B) was used to calculate the doubling time (Equation (3)). The calculated T_d was 60.3 days; however, this value depicts only an apparent biomass growth in the reactor and does not reflect the physiologically capacity of the N-damo microorganisms as growth substrates could have been a limiting factor during the reactor operation. Microbial growth rate is influenced by substrate limitation and higher growth rates are observed in a resource rich environment (Lipson, 2015). In our study, the permeate in MBR2 had a negligible average nitrite concentration of 0.35 $\pm$ 0.5 mg $NO^-_2 L^{-1}$ in the corresponding days (day 189–234), which suggests a nitrite limitation that could impact the growth kinetics and consequently the T_d.

$$\text{Linear equation for exponential growth } Y = Ae^{Bx} \quad (2)$$

$$\text{Doubling time } T_d = \ln(2)/B \quad (3)$$

The quantification of the biomass refers mainly to suspended flocs in the mixed liquor of the MBRs. However, the quantification does not include some remaining biomass adhered to the glass surface inside the MBRs as biofilms. Nevertheless, the excluded biomass fraction was not significant, and efforts were done to resuspend all the available biomass inside the MBRs continuously (i.e., Methane recirculation during the operation and nitrogen gas resuspension previous sampling to detach biofilm formation in the glass walls).

3.1.2. Biomass yield

The yield estimation (Y) considered the values from the last 70 days (PII and PIII) of MBR2 operation corresponding to the log phase in figure A2 (days 164–234) for quantifying the amount of biomass gained versus the amount of nitrite denitrified in the system (Equation (4)). The biomass gained was 1.76 g MLVSS L-1 and the nitrite removed accounted for 14.8 g N L^{-1} considering an average NLR of 211 mg $N–NO^-_2$ $L^{-1}d^{-1}$which resulted in an estimated yield of 0.12 g VSS g N^{-1} denitrified.

$$Yield\ \frac{(gBiomass)}{(gN\ denitrified)} = \frac{grBiomass\ earned}{(days * NLR)} \quad (4)$$

The calculated Y is similar to the estimated in previous N-damo studies (Guerrero-Cruz et al., 2019; Winkler et al., 2015) (Table 2). The Y represents a rough estimation of the process performance, contributing to the scarce knowledge on basic N-damo process parameters corresponding to high-rate operation. Generally, microorganisms that have high substrate consumption capacities have lower yields as there is usually a compensation regarding yield and substrate consumption (Ni et al., 2017). In this sense, the relative low yield of autotrophic N-damo compared to other heterotrophic microorganisms (i.e., the Y in heterotrophic denitrifiers is above 185 g VSS g N^{-1} (Ni et al., 2017)) result in lower sludge production and consequently, longer SRTs would be needed for its growth.

3.1.3. Evolution of the off-gas phase

The concentration of nitrous oxide, nitrogen, carbon dioxide and methane in the off gas were continuously measured by gas chromatography. The measurements showed that N_2O was absent most of the time during the reactor operation in both MBRs. In MBR1, the concentration

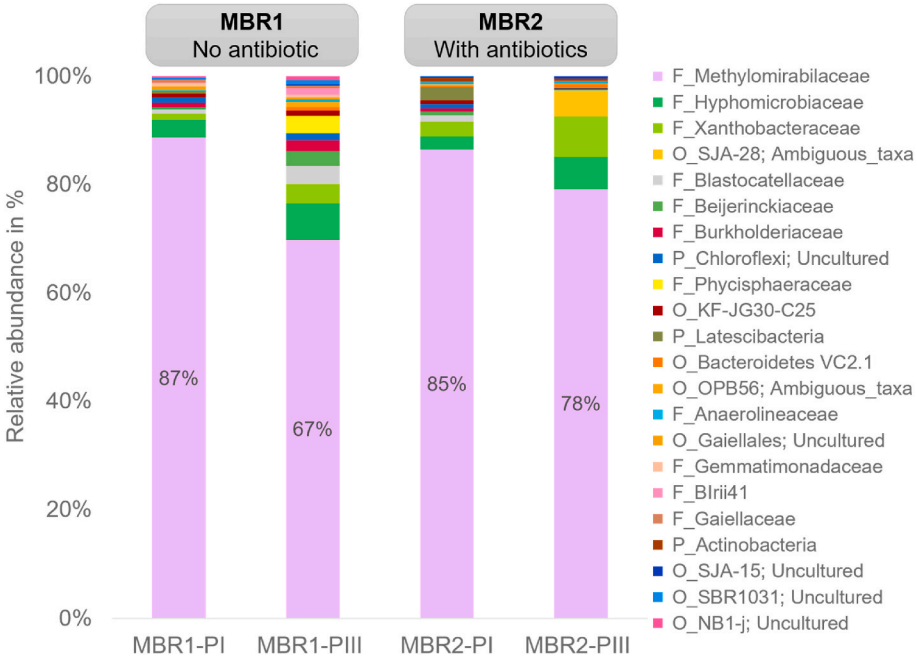

Fig. 2. Microbial communities are present in both MBR (MBR1 and MBR2) at the beginning (PI) and end of operation (PIII). The legend shows the respective taxonomic classification with the first letter: P_phylum, O_order, and F_family. Only taxon with relative abundances over 1% are represented. The shades of the same color identify microorganisms from the same order. (For interpretation of the references to color in this figure legend, the reader is referred to the Web version of this article.)

Table 2
Comparison of yield estimation with available literature (units recalculated).

Source	Yield (g VSS g N^{-1})
This study	0.12
Guerrero-Cruz et al. (2019)	0.13[a]
Winkler et al. (2015)	0.11[b]

[a] Assuming a stoichiometric relation 3/8 C:N during N-damo and a 50% C of the molecular biomass formula C5H8O2.3N1.1.
[b] Assuming a relation of 1.42 g COD g-1 VSS and 1.14 g COD g-1 N.

of N_2O was zero on 42 out of the 52 measurements performed in the reactor in the whole operation. In fact, in the first 203 days the average concentration was 0.02 mg N–N_2O L^{-1}, and N_2O was present in only three specific points with an average concentration of 19.88 mg N–N_2O L^{-1} during the last 30 operational days. In the case of MBR2, N_2O emissions were present only in the first 64 days of operation with an average concentration of 0.88 ± 0.9 mg N–N_2O L^{-1}. In the rest of the operation, N_2O emissions wero cero for 34 out of 37 measurements.

The specific measurements in which N_2O was found in both MBRs, corresponded to minor operational perturbances and to the presence of nitrite in the permeate. The few isolated peaks of N_2O identified corresponded to those moments in which there was a slight nitrite build up in the bioreactors, with concentrations below 3 mg N–NO_2^- L^{-1}. Considering the N-damo metabolism does not include N_2O as a process intermediate nor encodes the nitrous oxide reductase, the presence of trace concentrations of N_2O suggests the coexistence of conventional heterotrophic bacteria which includes N_2O as intermediate step as previously mentioned in similar reactor operation (Allegue et al., 2018; Arias et al., 2022). Moreover, it is also presumed that the specific medium composition used in this work, which has a reduction of salts (namely Ca, P and K) and the addition of EDTA (which enhances the Cu and Fe bioavailability), also favored the low/none N_2O emissions as previously demonstrated by Arias et al. (2022).

The values for methane, as it was fed in saturation, remained similar throughout the reactor operation accounting for about 80–87% of the biogas composition. The latter was influenced by the production of N_2 and presence of CO_2 that was about 5%.

3.1.4. Activity assays

Activity assays showed a high potential for nitrogen removal, with a maximum volumetric rate of 1332 mg N L-1d-1 and a specific nitrite removal rate as high as 540 mg N $gVSS^{-1}$ d^{-1} for PIII (Table 3). These values suggest that the N-damo process has the capability to remove nitrite at a practical useful rate, even comparable to the values observed by heterotrophic denitrification in full-scale installations (up to 420 mg $Ng^{-1}VSS$ d^{-1}); or even higher than other autotrophic process like Anammox (200 mg N g^{-1} VSS d^{-1}) (Lotti et al., 2015; Metcalf & Eddy et al., 2014). The maximum specific activity achieved in this study represent a step forward in the technological development of this process compared with previous values, which ranged from 64.13 mg N g^{-1} VSS d^{-1} (Arias et al., 2022), 95.53 mg N g^{-1} VSS d^{-1} (Allegue et al., 2018) to 186.3 mg N g^{-1} VSS d^{-1} (Martínez-Quintela et al., 2021). Other studies working with different technical approaches have reported considerable lower values, below 7 mg N g^{-1} VSS d^{-1} (Chang et al., 2021; He et al., 2015a; Hu et al., 2019).

The activity assays showed a maximum volumetric rate of 4-6-fold higher than the apparent volumetric rate measured during the continuous reactor operation (Table 3). The maximum activity values evidenced in this work are amongst the highest reported in literature, which in turn, supports the relevance of N-damo process for a successful technological application at large scale. Similarly, other studies using nitrite dependent N-damo enrichments have shown high volumetric rates up to 285.7 mg N g^{-1} L^{-1} d^{-1} (Arias et al., 2022). Moreover, enrichments combining Anammox, N-damo bacteria and N-damo archaea have shown values up to 330 mg N L^{-1} d^{-1} for nitrite removal (N-damo bacteria) and up to 684 for nitrate removal (N-damo archaea) (Cai et al., 2015).

3.2. Microbiological analysis

To understand the microbial community structure to the reactor functionality, the taxonomic analysis is discussed at a family level for a clearer comparison with previous work using similar reactors.

Relative abundances, showed that the N-damo population, represented by the *Methylomirabilaceae* family, dominated the microbial community during all reactor operation in both MBRs showing a relative abundance of up to 87% (Fig. 3). The N-damo bacteria, corroborates that the enrichment strategy (medium composition and reactor operation)

Table 3
Maximum activity tests result for all experimental periods.

Period	Activity Assays[a]			Continuous Reactor Operation		
	Suspended biomass	Maximum activity	Maximum volumetric rate	Apparent volumetric rate	Average nitrite in permeate	Suspended biomass
	g VSS L^{-1}	mgN-NO^-_2 g^{-1} VSS d^{-1}	mgN-NO^-_2 L^{-1} d^{-1}	mgN-NO^-_2 L^{-1} d^{-1}	mgN-NO^-_2 L^{-1} d^{-1}	g VSS L^{-1}
I	1.32	245	323	75.84 ± 10.01	1.01 ± 2.10	1.27 ± 0.10
II	1.38	486	672	161.48 ± 11.41	0.11 ± 0.02	1.40 ± 0.07
III	2.47	540	1332	215.21 ± 24.22	0.38 ± 0.50	2.27 ± 0.48

[a] Activity assays were performed in MBR2.

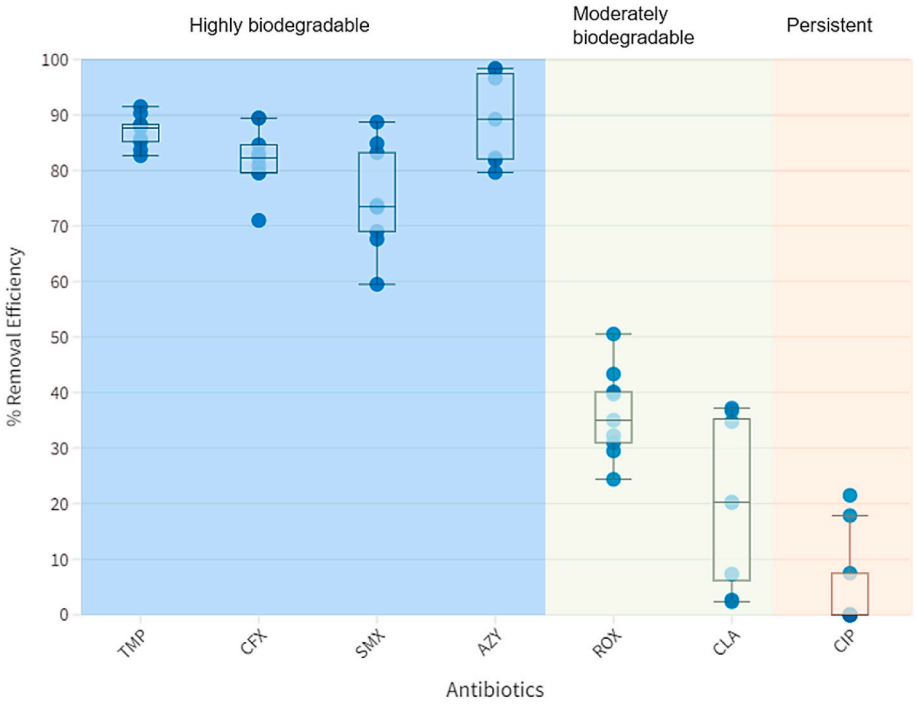

Fig. 3. Overall removal efficiencies of selected antibiotics. Each compound was measured in MBR2 in all three experimental periods in triplicates when MBR2 (n = 9, except for CIP that only included positive removals). Error bars show standard variations. The colored background helps identify the three removal tendencies observed: Highly biodegradable, moderately biodegradable, and persistent.

was efficient in cultivating N-damo bacteria. The N-damo bacteria population achieved for both MBRs surpasses previous enrichments strategies using a similar MBRs where a maximum abundance of 57% was evidenced (Arias et al., 2022). The incorporation of the lanthanide Cerium in the feeding composition is hypothesized to have boosted the growth of the N-damo culture and influenced the adaptation of the microbial community to high NLRs. Similarly, previous studies have supplemented their NC10 enrichment culture with the lanthanide Cerium to release a potential growth limitations successfully (Versantvoort et al., 2018). This is mainly because many methylotrophs can use Cerium instead of Calcium as cofactor for the activation of the enzyme methanol dehydrogenase (MDH) (Guerrero-Cruz et al., 2019). This is particularly relevant, as it is suggested that lanthanides can provide superior catalytic properties for the respective enzymatic function (Pol et al., 2014).

Interestingly, the N-damo population, although predominant, suffered a significant decrease with the increase in NLR, this trend was observed in both MBRs. In Period III, the family *Methylomirabilaceae* decreased from 87% to 67% and from 85% to 78% of relative abundance in MBR1 and MBR2, respectively (Fig. 3). The decrease of the predominant N-damo family was concomitant with the increase in abundance of minor species present in both reactors. Particularly, microorganisms from the Order Rizhobiales depicted by the families *Hyphomicrobiaceae* and *Xanthobacteraceae* increased their abundance in both MBRs (Fig. 4). Specifically in the case of MBR2, microorganisms from the order SJA-28 were distinctly favored in period III.

Microorganisms belonging to the family *Xanthobacteraceae* are known to be facultative chemolithoautotrophy with hydrogen and/or reduced sulfur compounds and to have the hability to fix N_2 (Oren, 2014). Moreover, some family representatives have been involved in the cometabolic degradation of different OMPs chlorinated alkanes (Ensign et al., 1992) and antibiotics, particularly SMX (Yang et al., 2020) which suggest potential biotechnological applications. In fact, several species (*Xanthobacter autotrophicus, X. flavus, Labrys methylaminiphilus* and others) have been shown resistant to antibiotics such as ampicillin, chloramphenicol, erythromycin, penicillin and tetracycline (Oren, 2014).

The increase of the *Hyphomicrobiaceae family* in both MBRs at higher NLRs (Fig. 4) can be explained by the simultaneous decrease in N-damo population and the respective loss of reverse methanogenenic activity. Members from the *Hyphomicrobiaceae* family (belonging to the *Hyphomicrobium* genus) have been characterized as methylotrophs involved in methanol-fed denitrification systems (Rissanen et al., 2016). Similarly, another study has shown that *Hyphomicrobiaceae* is a key bacterial population involved in methane-dependent denitrification (Osaka et al., 2008). Therefore, the loss of N-damo population would provide less

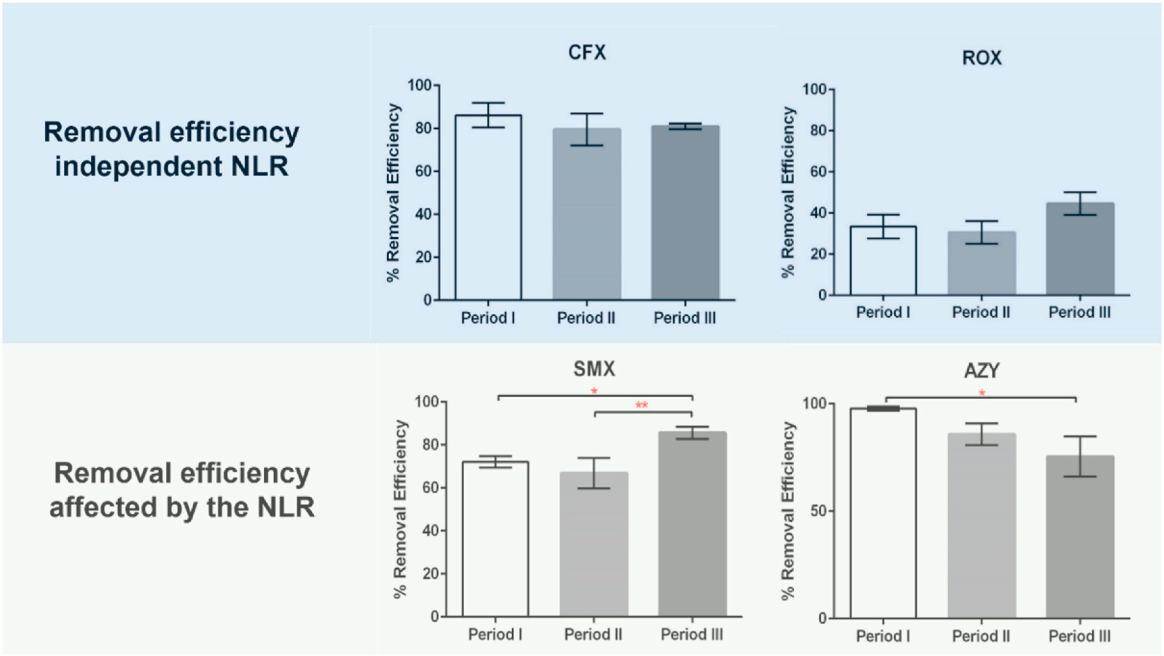

Fig. 4. Average removal efficiency in each period. Above, CFX and ROX as compounds which were not affected by the NLR. Below, SMX and AZY as compounds who were affected with the NLR. The asterisks highlight those antibiotics whose removal efficiencies are significantly different among periods ($p \leq 0.05$) by a One-way Anova and Tukey's multiple comparison test. Error bars show standard variation ($n = 3$).

substrate competition for the methane oxidation and thus potentially provide an opportunity for other methanotrophs to thrive.

Previous N-damo studies at low NLR, also identified a significant presence of microorganisms from the order SJA-28 that showed opposite temporal behavior to the *Methylomirabiliaceae* family (Allegue et al., 2018). In the former study, as the MBRs were increasing in NLRs and in simultaneous the abundance of N-damo bacteria, microorganisms from SJA-28 declined, which suggested an alternating relationship between both microorganisms. In this study, NLRs were distinctly higher and reactor efficiency was not altered, however, we evidenced the same opposing tendency as SJA-28 abundance increased with the decreased in N-damo. Based on all the above, it appears that both groups of microorganisms have an intrinsic relationship that ultimately impacts the community structure. However, it remains unclear why only MBR2 showed a significative increase of the order SJA-28 and MBR1did not show a negligible presence despite having the same NLRs and similar initial microbial compositions (Fig. 3). In this sense, although SJA-28 is a relatively unknown taxon, it is possible that the increase might be related with the presence of antibiotics.

Regarding the influence of antibiotic presence, the similarity in the microbial composition of both in PI for both MBRs suggests that microbial shifts were not immediate but rather visible after long-term exposure to environmental concentrations of antibiotics (Fig. 3). At the end of the reactor operation (PIII), Shannon diversity index increased for MBR1, but decreased for MBR2 (Table A2) despite having similar NRLs (Fig. 1). These results suggest two possible assertions, firstly, higher NLRs during N-damo demand for more diversity in the microbial community structure to be able to maintain reactor efficiency. And secondly, the presence of antibiotics causes an impact on the diversity of the community composition, especially observed at long-term operation (MBR1-PIII vs. MBR2-PIII) (Figure A3).

3.3. Removal of antibiotics

Based on the overall extent of their biotransformation, the selected antibiotics can be classified in three trends due to their average removals across the operation: i) highly biodegradable: TMP (83% ± 7.9), CFX (82% ± 2.1), SMX (75% ± 2.1) and AZY (86% ± 9.1); ii) moderately biodegradable: ROX (36% ± 6.0) and CLA (24% ± 15.4); and iii) persistent CIP (0%) (Fig. 3).

For the highly biodegradable compounds, two behaviors were observed, i) high and stable removal, which was independent of the changes of operational conditions and microbial dynamic composition (TMP and CFX) and ii) compounds with wider variations in their removal as occurred with SMX and AZY (Fig. 4).

CFX was efficiently removed in all operation periods with an average removal of 82 ± 6%. Although the information about its removal under anoxic conditions is scarce, previous works operating with other conditions (aerobic activated sludges, concentrations of 100 μg CFX L^{-1}) reported almost total biodegradation (97%), with a biodegradation constant rate (k_{biol}) of 0.36 h^{-1} (Li and Zhang, 2010). CFX, as most β-lactams, is easily biodegraded during biological wastewater treatment due the cleavage of its unstable β-lactam ring by the activity of β-lactamases, a group of enzymes widely excreted in wastewater microbiomes (Liu et al., 2021; Oberoi et al., 2019).

In the case of TMP, efficiencies obtained in this work were quite high (87 ± 3%) and stable. Previous works in anoxic conditions, showed significantly lower values, with removal efficiencies below 20% (Martínez-Quintela et al., 2021; Suarez et al., 2010). The increased removal efficiency in our work could be explained by the significantly higher biomass activities used compared to the other authors.

Similarly, the removal efficiencies obtained for SMX were high during all operation but particularly in PIII (85–90%), which showed a significative increase with respect PI and PII (Fig. 4). These results are quite different from those obtained in conventional heterotrophic denitrification, where SMX was considered persistent, with removals below 26% (Suarez et al., 2010). Other MBBRs studies using methanol/ethanol dosing as carbon source reported biodegradability of SMX up 50%, operating at a very low SMX concentration 0.04 μg L^{-1} (Torresi et al., 2017). Previous N-damo studies indicated SMX could be removed up to 62% (Martínez-Quintela et al., 2020). In our study, the maximum specific removal rate was 2.2 μg SMX g^{-1}VSS d^{-1} reached in period I (at 76 mg N $L^{-1}d^{-1}$). In a similar manner, Martínez-Quintela et al. (2020), reached a maximum specific removal of 1.8 μg SMX g^{-1} VSS d^{-1} at 50

mg N L^{-1} d^{-1}. Despite the significative increase in average removal in PIII with PII and PI, there was no increase in specific SMX removal rate. These results suggest that the growth of biomass was not directly functional for SMX removal but rather to the nitrite removal.

With regards to the macrolide AZY, the information about its fate in anoxic conditions is scarce. Our results show a high biodegradability (75–97%) (Fig. 3), but with a decreasing tendency in the long-term operation (Fig. 4). Similarly, as with SMX, the specific removal of AZY was not enhanced as the biomass activity increased. In PI, the average specific removal was 3.45 μg AZY g^{-1} VSS d^{-1} and in PIII, this value dropped until 1.70 μg AZY g^{-1} VSS d^{-1}. Previous works under aerobic conditions using environmental relevant concentrations from 0.1 to 13 μg L^{-1} report removal efficiencies around 50% using activated sludge (Abegglen et al., 2009; Blair et al., 2015) or MBRs (Abegglen et al., 2009).

For these four highly biodegradable OMPs, a positive tendency between antibiotic removal and NRL were evidenced mainly for SMX (Fig. 4). However, decreasing tendencies were observed when considering the specific antibiotic removal and the specific denitrifying activity for SMX and AZY (Figure A4). Several explanations have been given to explain this different behavior respect to the cometabolic tendency of OMPs during N-damo at lower NLR (Martínez-Quintela et al., 2021). One of them is referred to the HRT used, 1 d in this work, which can be high enough to hide the cometabolic effect showing the same removal for operational periods (Kennes-Veiga et al., 2021). On the other hand, the exponential increase in biomass concentration observed in PII and PIII could suggest that the microbial growth was especially linked to microorganisms involved in N removal more than the species related to OMP biotransformation, which finally caused a shift in the microbial community composition (Figure A3). Another factor that should be considered is the difficulty for an accurate quantification of the biomass present as biofilm in the system (only suspended has been measured), which might underestimate real biomass concentrations inside the reactors.

Besides these considerations, other factors, such as the evolution of the microbial composition in the MBRs should be considered. In this way, microbiological analysis revealed a 7% reduction of the N-Damo culture in MBR2 (relative abundance of *Methylomirabilaceae* family (Fig. 3), along with the increase of NLR applied during the reactor operation. The negative trend between biotransformation and specific biomass activity (especially observed in AZY) might be explained by a reduction in the functional population involved in the biotransformation of both SMX and AZY. In the same manner, previous research links the potential biotransformation capacity to the presence of the key enzyme methane monooxygenase (MMO) (present in N-damo) which is suggested to be capable of target OMP functional groups (Jiang et al., 2010; Wang et al., 2022).

In the case of moderately biotransformed antibiotics, the macrolides ROX and CLA, results showed hardly any increase in removal efficiency nor specific OMP removal despite the increase in NLRs (i.e., N-damo activity) (Fig. 4). The moderate removal of ROX was also evidenced by Suarez et al. (2010) during heterotrophic denitrification, where the removal of ROX accounted for less than 20% (using 20 μg L^{-1} as initial concentration). On the other hand, CLA was removed between 4 up to 42% with a decline in efficiency in period II. Although there are no information in anoxic conditions, previous research has also shown moderate removal of CLA (30–55%) during aerobic biological removal ($C_{initial}$ = 14 μg L^{-1}) (Escolà Casas et al., 2015). From these results, it appears that in both systems the maximum kinetics capacity (i.e., k_{biol}) for the biotransformation of both compounds has been achieved, which can be explained either by the achievement of the saturation level at these concentrations or because of thermodynamic constraints (chemical equilibrium or enzymatic reversibility) (Gonzalez-gil et al., 2018; Kennes-Veiga et al., 2022; Sheng et al., 2021).

CIP was persistent throughout all the reactor operation. Similarly, Dorival-García et al. (2013), evidenced less than 5% removal of CIP ($C_{initial}$ = 500 μg L^{-1}), suggesting a recalcitrant behavior of CIP in anoxic conditions. Even though the presence of antibiotics did not show any inhibitory effects in this study, CIP was also found to be recalcitrant to biodegradation in water and soil samples while also strongly inhibiting the microbial activities (Girardi, 2011). The persistence of CIP to biodegradation could be explained by its zwitterionic behavior, which suggests that biodegradation is a secondary removal route and CIP is mainly removed by sorption (Dorival-García et al., 2013).

Although most of the selected antibiotics were highly removed in the N-damo MBR system, the specific OMP removal did not correlate with the specific denitrifying activity. For most compounds, higher NLRs did not significantly enhance antibiotic biotransformation, at least when operating at 1 d of HRT. Microbiological factors, such as differences in taxonomic composition, including the abundance of N-damo bacteria as functional microorganisms might be having more influence on the biotransformation mechanism of the selected compounds.

Previous research has evidenced shifts in microbial community composition associated solely by the presence of OMPs even at environmental relevant concentrations (Li et al., 2020; Zou et al., 2021). For example, the presence of 50 μg L^{-1} of CIP has been linked to the decrease of proteobacteria from 44% to 36% (Li et al., 2020). Other authors evidenced that denitrifying bacteria are particularly sensitive to trace concentrations of CIP or similar fluoroquinolones (even at ng L^{-1} level) (Yi et al., 2017; Zou et al., 2021).

Combining all results, it appears that the microbials shifts happening in the MBRs have a greater impact on antibiotic biotransformation than the primary metabolism associated to the NLRs. The negative tendencies of specific antibiotic removal observed (namely on SMX and AZY) might be explained by the decline of the functional N-damo bacteria, associated to the M*ethylomirabilaceae* family.

4. Conclusions

A stable and long-term MBR operation with high NRRs (up to mg220 $N–NO^{-}_{2}L$-1) was achieved. Moreover, N-damo activity evidenced an even higher nitrite removal potential of up to 540 mg $N–NO^{-}2$ g^{-1} VSS d^{-1} during the maximum activity assays performed. This values, jointly with the reactor stability and robustness to high nitrogen load increase, constitutes an important progress for its technological applicability.

The *Methylomirabiliaceae* family dominated the microbial community with a relative abundance of up to 87% during stable reactor operation. However, it appears that high NLRs seem to favour the growth of minor species present in the community (namely from the order Rizhobiales).

Most of the antibiotics were biotransformed except for CIP that showed persistent behavior. CFX, TMP, SMX and AZY were highly biotransformed in the average range of 74–89% and in the case of ROX and CLA, a moderate biotransformation with average values of 20–36% across all NLRs was observed. The increase in biomass activity (in PII and PIII) did not enhance the removal efficiency, as highest removals were observed in PI. Moreover, it seems that the shifts in microbial community composition due to the different NLRs appears to have a greater impact for the removal of the studied antibiotics.

Combining all evidence, it appears that N-damo microorganisms seem to be functionally involved in the biotransformation of the selected antibiotics, and their decrease seems to affect the removal efficiency of the system, especially in the case of AZY.

Credit author statement

Silvana Quiton-Tapia: Conceptualization, Methodology, Formal analysis, Investigation, Data curation, Writing - Original Draft, Writing - Review & Editing, and Visualization. **Sabela Balboa:** Methodology, Formal analysis, Data curation and Writing - Review & Editing. **Francisco Omil:** Conceptualization, Methodology, Data curation, Writing - Review & Editing, Visualization, Supervision and Funding acquisition.

Juan Manuel Garrido: Conceptualization, Methodology, Data curation, Writing - Review & Editing, Visualization and Supervision. **Sonia Suárez:** Conceptualization, Methodology, Data curation, Writing - Review & Editing, Visualization, Supervision and Funding acquisition.

Declaration of competing interest

The authors declare that they have no known competing financial interests or personal relationships that could have appeared to influence the work reported in this paper.

Data availability

Data will be made available on request.

Acknowledgements

This research was supported by the European Union's Horizon 2020 research and innovation programme under the project NOWELTIES, through the Marie Sklodowska-Curie grant agreement 812880, as well as the Ministry of Economy and Competitiveness, Spain through ANTARES (PID 2019-110346RB-C21) project. Authors belong to CRETUS Strategic Partnership (AGRUP 2015/02) and to Galician Competitive Research Group (GRC ED431C-2021/37).

Appendix A. Supplementary data

Supplementary data to this article can be found online at https://doi.org/10.1016/j.envpol.2023.122033.

References

Abegglen, C., Joss, A., McArdell, C.S., Fink, G., Schlüsener, M.P., Ternes, T.A., Siegrist, H., 2009. The fate of selected micropollutants in a single-house MBR. Water Res. 43, 2036–2046. https://doi.org/10.1016/j.watres.2009.02.005.

Allegue, T., Arias, A., Fernandez-Gonzalez, N., Omil, F., Garrido, J.M., 2018. Enrichment of nitrite-dependent anaerobic methane oxidizing bacteria in a membrane bioreactor. Chem. Eng. J. 347, 721–730. https://doi.org/10.1016/j.cej.2018.04.134.

Alvarino, T., Suarez, S., Lema, J.M., Omil, F., 2014. Understanding the removal mechanisms of PPCPs and the influence of main technological parameters in anaerobic UASB and aerobic CAS reactors. J. Hazard Mater. 278, 506–513. https://doi.org/10.1016/j.jhazmat.2014.06.031.

APHA, 2000. Standard Methods for the Examination of Water and Wastewater, twentieth ed. https://doi.org/10.5860/choice.37-2792

Arias, A., Allegue, T., Darwich, A., Fachal-Suarez, M., Martínez-quintela, M., Omil, F., Garrido, J.M., 2022. Operating Strategies to Optimize a Membrane Bioreactor Enriched in Nitrite-dependent Anaerobic Methane-Oxidizing Bacteria 450. https://doi.org/10.1016/j.cej.2022.138289.

Blair, B., Nikolaus, A., Hedman, C., Klaper, R., Grundl, T., 2015. Evaluating the degradation, sorption, and negative mass balances of pharmaceuticals and personal care products during wastewater treatment. Chemosphere 134, 395–401. https://doi.org/10.1016/j.chemosphere.2015.04.078.

Cai, C., Hu, S., Guo, J., Shi, Y., Xie, G.J., Yuan, Z., 2015. Nitrate reduction by denitrifying anaerobic methane oxidizing microorganisms can reach a practically useful rate. Water Res. 87, 211–217. https://doi.org/10.1016/j.watres.2015.09.026.

Chang, J., Wu, Q., Yan, X., Wang, H., Lee, L.W., Liu, Y., Liang, P., Qiu, Y., Huang, X., 2021. Enhancement of nitrite reduction and enrichment of Methylomonas via conductive materials in a nitrite-dependent anaerobic methane oxidation system. Environ. Res. 193, 110565 https://doi.org/10.1016/j.envres.2020.110565.

Dorival-García, N., Zafra-Gómez, A., Navalón, A., González-López, J., Hontoria, E., Vílchez, J.L., 2013. Removal and degradation characteristics of quinolone antibiotics in laboratory-scale activated sludge reactors under aerobic, nitrifying and anoxic conditions. J. Environ. Manag. 120, 75–83. https://doi.org/10.1016/j.jenvman.2013.02.007.

Ensign, S.A., Hyman, M.R., Arp, D.J., 1992. Cometabolic degradation of chlorinated alkenes by alkene monooxygenase in a propylene-grown Xanthobacter strain. Appl. Environ. Microbiol. 58, 3038–3046. https://doi.org/10.1128/aem.58.9.3038-3046.1992.

Escolà Casas, M., Chhetri, R.K., Ooi, G., Hansen, K.M.S., Litty, K., Christensson, M., Kragelund, C., Andersen, H.R., Bester, K., 2015. Biodegradation of pharmaceuticals in hospital wastewater by a hybrid biofilm and activated sludge system (Hybas). Sci. Total Environ. 530–531, 383–392. https://doi.org/10.1016/j.scitotenv.2015.05.099.

Ettwig, K.F., Butler, M.K., Le Paslier, D., Pelletier, E., Mangenot, S., Kuypers, M.M.M., Schreiber, F., Dutilh, B.E., Zedelius, J., De Beer, D., Gloerich, J., Wessels, H.J.C.T., Van Alen, T., Luesken, F., Wu, M.L., Van De Pas-Schoonen, K.T., Op Den Camp, H.J.M., Janssen-Megens, E.M., Francoijs, K.J., Stunnenberg, H., Weissenbach, J., Jetten, M.S.M., Strous, M., 2010. Nitrite-driven anaerobic methane oxidation by oxygenic bacteria. Nature 464, 543–548. https://doi.org/10.1038/nature08883.

Girardi, C., 2011. Comparison of the Biodegradation of Pharmaceuticals and Biocides in Water and Soil Systems 142.

Gonzalez-gil, L., Mauricio-iglesias, M., Carballa, M., Lema, J.M., 2018. Why are organic micropollutants not fully biotransformed ? A mechanistic modelling approach to anaerobic systems. Water Res. 142, 115–128. https://doi.org/10.1016/j.watres.2018.05.032.

Gros, M., Rodríguez-Mozaz, S., Barceló, D., 2013. Rapid analysis of multiclass antibiotic residues and some of their metabolites in hospital, urban wastewater and river water by ultra-high-performance liquid chromatography coupled to quadrupole-linear ion trap tandem mass spectrometry. J. Chromatogr. A 1292, 173–188. https://doi.org/10.1016/j.chroma.2012.12.072.

Guerrero-Cruz, S., Stultiens, K., van Kessel, M.A.H.J., Versantvoort, W., Jetten, M.S.M., Op den Camp, H.J.M., Kartal, B., 2019. Key physiology of a nitrite-dependent methane-oxidizing enrichment culture. Appl. Environ. Microbiol. 1–9.

He, Z., Geng, S., Shen, L., Lou, L., Zheng, P., Xu, X., Hu, B., 2015a. The short- and long-term effects of environmental conditions on anaerobic methane oxidation coupled to nitrite reduction. Water Res. 68, 554–562. https://doi.org/10.1016/j.watres.2014.09.055.

He, Z., Wang, J., Zhang, X., Cai, C., Geng, S., Zheng, P., Xu, X., Hu, B., 2015b. Nitrogen removal from wastewater by anaerobic methane-driven denitrification in a lab-scale reactor: heterotrophic denitrifiers associated with denitrifying methanotrophs. Appl. Microbiol. Biotechnol. 99, 10853–10860. https://doi.org/10.1007/s00253-015-6939-9.

Hu, Z., Ru, D., Wang, Y., Zhang, J., Jiang, L., Xu, X., Nie, L., 2019. Optimization of a nitrite-dependent anaerobic methane oxidation (n-damo) process by enhancing methane availability. Bioresour. Technol. 275, 101–108. https://doi.org/10.1016/j.biortech.2018.12.035.

Jiang, H., Chen, Y., Jiang, P., Zhang, C., Smith, T.J., Murrell, J.C., Xing, X.H., 2010. Methanotrophs: multifunctional bacteria with promising applications in environmental bioengineering. Biochem. Eng. J. 49, 277–288. https://doi.org/10.1016/j.bej.2010.01.003.

Kampman, C., Hendrickx, T.L.G., Luesken, F.A., van Alen, T.A., Op den Camp, H.J.M., Jetten, M.S.M., Zeeman, G., Buisman, C.J.N., Temmink, H., 2012. Enrichment of denitrifying methanotrophic bacteria for application after direct low-temperature anaerobic sewage treatment. J. Hazard Mater. 227–228, 164–171. https://doi.org/10.1016/j.jhazmat.2012.05.032.

Kennes-Veiga, D.M., Gonzalez-Gil, L., Carballa, M., Lema, J.M., 2021. The organic loading rate affects organic micropollutants' cometabolic biotransformation kinetics under heterotrophic conditions in activated sludge. Water Res. 189, 116587 https://doi.org/10.1016/j.watres.2020.116587.

Kennes-Veiga, D.M., Gónzalez-Gil, L., Carballa, M., Lema, J.M., 2022. Enzymatic cometabolic biotransformation of organic micropollutants in wastewater treatment plants: a review. Bioresour. Technol. 344 https://doi.org/10.1016/j.biortech.2021.126291.

Li, B., Zhang, T., 2010. Biodegradation and adsorption of antibiotics in the activated sludge process. Environ. Sci. Technol. 44, 3468–3473. https://doi.org/10.1021/es903490h.

Li, X., Lu, S., Liu, S., Zheng, Q., Shen, P., Wang, X., 2020. Shifts of bacterial community and molecular ecological network at the presence of fluoroquinolones in a constructed wetland system. Sci. Total Environ. 708, 135156 https://doi.org/10.1016/j.scitotenv.2019.135156.

Lipson, D.A., 2015. The complex relationship between microbial growth rate and yield and its implications for ecosystem processes. Front. Microbiol. 6, 1–5. https://doi.org/10.3389/fmicb.2015.00615.

Liu, C., Tan, L., Zhang, L., Tian, W., Ma, L., 2021. A review of the distribution of antibiotics in water in different regions of China and current antibiotic degradation pathways. Front. Environ. Sci. 9, 1–24. https://doi.org/10.3389/fenvs.2021.692298.

Lotti, T., Kleerebezem, R., van Loosdrecht, M.C.M., 2015. Effect of temperature change on anammox activity. Biotechnol. Bioeng. 112, 98–103. https://doi.org/10.1002/bit.25333.

Luesken, F.A., Sa, J., Alen, T.A., Van, Sanabria, J., Camp, H.J.M., Den, O., Jetten, M.S.M., Kartal, B., 2011. Simultaneous Nitrite-dependent Anaerobic Methane and Ammonium Oxidation Processes ᴑ 77, pp. 6802–6807. https://doi.org/10.1128/AEM.05539-11.

Martínez-Quintela, M., Arias, A., Alvarino, T., Suarez, S., Garrido, J.M., Omil, F., 2021. Cometabolic removal of organic micropollutants by enriched nitrite-dependent anaerobic methane oxidizing cultures. J. Hazard Mater. 402, 123450 https://doi.org/10.1016/j.jhazmat.2020.123450.

Metcalf & Eddy, Tchobanoglous, G., Burton, F.L., Stensel, H.D., 2014. Wastewater Engineering. Treatment and Resource Recovery, Fifth. Ed.

Ni, B.J., Pan, Y., Guo, J., Virdis, B., Hu, S., Chen, X., Yuan, Z., 2017. Chapter 16: denitrification processes for wastewater treatment. In: RSC Metallobiology. The Royal Society of Chemistry. https://doi.org/10.1039/9781782623762-00368.

Oberoi, A.S., Jia, Y., Zhang, H., Khanal, S.K., Lu, H., 2019. Insights into the fate and removal of antibiotics in engineered biological treatment systems: a critical review. Environ. Sci. Technol. 53, 7234–7264. https://doi.org/10.1021/acs.est.9b01131.

Oren, A., 2014. The prokaryotes: alphaproteobacteria and betaproteobacteria. In: Rosenberg, E., DeLong, E.F., Lory, S., Stackebrandt, E., Thompson, F. (Eds.), The Family Xanthobacteraceae. The Prokaryotes. Springer Berlin Heidelberg, pp. 1–1012. https://doi.org/10.1007/978-3-642-30197-1.

Osaka, T., Ebie, Y., Tsuneda, S., Inamori, Y., 2008. Identification of the bacterial community involved in methane-dependent denitrification in activated sludge using

DNA stable-isotope probing. FEMS Microbiol. Ecol. 64, 494–506. https://doi.org/10.1111/j.1574-6941.2008.00473.x.

Pol, A., Barends, T.R.M., Dietl, A., Khadem, A.F., Eygensteyn, J., Jetten, M.S.M., Op den Camp, H.J.M., 2014. Rare earth metals are essential for methanotrophic life in volcanic mudpots. Environ. Microbiol. 16, 255–264. https://doi.org/10.1111/1462-2920.12249.

Rissanen, A.J., Ojala, A., Dernjatin, M., Jaakkola, J., Tiirola, M., 2016. Methylophaga and Hyphomicrobium can be used as target genera in monitoring saline water methanol-utilizing denitrification. J. Ind. Microbiol. Biotechnol. 43, 1647–1657. https://doi.org/10.1007/s10295-016-1839-2.

Sánchez, A., Rodríguez-Hernández, L., Buntner, D., Esteban-García, A.L., Tejero, I., Garrido, J.M., 2016. Denitrification coupled with methane oxidation in a membrane bioreactor after methanogenic pre-treatment of wastewater. J. Chem. Technol. Biotechnol. 91, 2950–2958. https://doi.org/10.1002/jctb.4913.

Sheng, Q., Yi, M., Men, Y., Lu, H., 2021. Cometabolism of 17α-ethynylestradiol by nitrifying bacteria depends on reducing power availability and leads to elevated nitric oxide formation. Environ. Int. https://doi.org/10.1016/j.envint.2021.106528.

Stein, L.Y., 2020. The long-term relationship between microbial metabolism and Greenhouse Gases. Trends Microbiol. 28, 500–511. https://doi.org/10.1016/j.tim.2020.01.006.

Suarez, S., Lema, J.M., Omil, F., 2010. Removal of pharmaceutical and personal care products (PPCPs) under nitrifying and denitrifying conditions. Water Res. 44, 3214–3224. https://doi.org/10.1016/j.watres.2010.02.040.

Torresi, E., Escolà Casas, M., Polesel, F., Plósz, B.G., Christensson, M., Bester, K., 2017. Impact of external carbon dose on the removal of micropollutants using methanol and ethanol in post-denitrifying Moving Bed Biofilm Reactors. Water Res. 108, 95–105. https://doi.org/10.1016/j.watres.2016.10.068.

Tran, N.H., Urase, T., Ngo, H.H., Hu, J., Ong, S.L., 2013. Insight into metabolic and cometabolic activities of autotrophic and heterotrophic microorganisms in the biodegradation of emerging trace organic contaminants. Bioresour. Technol. 146, 721–731. https://doi.org/10.1016/j.biortech.2013.07.083.

van Kessel, M.A., Stultiens, K., Slegers, M.F., Guerrero Cruz, S., Jetten, M.S., Kartal, B., Op den Camp, H.J., 2018. Current perspectives on the application of N-damo and anammox in wastewater treatment. Curr. Opin. Biotechnol. 50, 222–227. https://doi.org/10.1016/j.copbio.2018.01.031.

Versantvoort, W., Guerrero-Cruz, S., Speth, D.R., Frank, J., Gambelli, L., Cremers, G., van Alen, T., Jetten, M.S.M., Kartal, B., Op den Camp, H.J.M., Reimann, J., 2018. Comparative genomics of Candidatus Methylomirabilis species and description of Ca. Methylomirabilis lanthanidiphila. Front. Microbiol. 9, 1–10. https://doi.org/10.3389/fmicb.2018.01672.

Wang, J., Zhang, C., Poursat, B.A.J., de Ridder, D., Smidt, H., van der Wal, A., Sutton, N. B., 2022. Unravelling the contribution of nitrifying and methanotrophic bacteria to micropollutant co-metabolism in rapid sand filters. J. Hazard Mater. 424, 127760 https://doi.org/10.1016/j.jhazmat.2021.127760.

Winkler, M.H., Ettwig, K.F., Vannecke, T.P.W., Stultiens, K., Bogdan, A., Kartal, B., Volcke, E.I.P., 2015. ScienceDirect Modelling simultaneous anaerobic methane and ammonium removal in a granular sludge reactor. Water Res. 73, 323–331. https://doi.org/10.1016/j.watres.2015.01.039.

Wolff, D., Krah, D., Dötsch, A., Ghattas, A.K., Wick, A., Ternes, T.A., 2018. Insights into the variability of microbial community composition and micropollutant degradation in diverse biological wastewater treatment systems. Water Res. 143, 313–324. https://doi.org/10.1016/j.watres.2018.06.033.

Yang, C.W., Liu, C., Chang, B.V., 2020. Biodegradation of amoxicillin, tetracyclines and sulfonamides in wastewater sludge. Water (Switzerland) 12. https://doi.org/10.3390/W12082147.

Yi, K., Wang, D., Yang, Qi, Li, X., Chen, H., Sun, J., An, H., Wang, L., Deng, Y., Liu, J., Zeng, G., 2017. Effect of ciprofloxacin on biological nitrogen and phosphorus removal from wastewater. Sci. Total Environ. 605 (606), 368–375. https://doi.org/10.1016/j.scitotenv.2017.06.215.

Zou, H., He, J., Guan, X., Zhang, Y., Deng, L., Li, Y., Liu, F., 2021. Microbial responses underlying the denitrification kinetic shifting exposed to ng/L- and μg/L-level lomefloxacin in groundwater. J. Hazard Mater. 417 https://doi.org/10.1016/j.jhazmat.2021.126093.